

“To Study about single input multiple output in power electronics”

Pandav Prakashkumar I

Tatva Institute of Technological Studies

Department of Electrical Engineering (Power system), Modasa, Gujarat

Abstract— The aim of this study is to develop a high-efficiency single-input multiple-output (SIMO) dc–dc converter. The proposed converter can boost the voltage of a low-voltage input power source to a controllable high-voltage dc bus and middle-voltage output terminals. The high-voltage dc bus can take as the main power for a high-voltage dc load or the front terminal of a dc–ac inverter. Moreover, middle-voltage output terminals can supply powers for individual middle-voltage dc loads or for charging auxiliary power sources (e.g., battery modules). In this study, a coupled-inductor based dc–dc converter scheme utilizes only one power switch with the properties of voltage clamping and soft switching, and the corresponding device specifications are adequately designed. As a result, the objectives of high-efficiency power conversion, high step up ratio, and various output voltages with different levels can be obtained. Some experimental results via a kilowatt-level prototype are given to verify the effectiveness of the proposed SIMO dc–dc converter in practical applications.

Index Terms- Coupled inductor, single-input multiple-output (SIMO) converter, soft switching, voltage clamping, MOSFET, VSI, PWM, ZCS, HVSC

I. INTRODUCTION

Multiple output converters are widely used in the industrial applications. Designing multi-output converters presents a remarkable challenge for the power supply designer. Converters utilizing a single primary power stage and generating more than one isolated output voltage are called multi-output converters. The basic requirements are small size and high efficiency. High switching frequency is necessary for achievement of small size. If the switching frequency is increased then the switching loss will increase. This decreases the efficiency of the power supplies. To solve this problem, some kinds of soft switching techniques need to be used to operate under high switching frequency. Zero Voltage Switched (ZVS) technique and Zero Current Switched (ZCS) technique are two commonly used soft switching methods. By using these techniques, either voltage or current is zero during switching transition, which largely reduce the switching loss and also increase the reliability for the power supplies.

Applications may require step-up, or at times even a bipolar supply from the same battery supply. Bipolar supplies also find a wide range of application in organic light emitting diodes. As a result, the design of a power management IC typically comprises boost to step-up, buck-boost to generate negative supply, and linear regulators to meet different supplies for various circuit applications. Several methods have been proposed to regulate the multiple outputs, to reduce the conduction loss, the MOSFET switch with low turn-on resistance is used; dc–dc converters are widely used in low and high-power applications. Patra *et al.* [1] presented a SIMO dc–dc converter capable of simultaneously generating buck, boost, and inverted outputs. However, over three switches for one output were required. This scheme is only suitable for the low output voltage and power application, and its power conversion is degenerated due to the operation of hard switching. Nami *et al.*[2] proposed a new dc–dc multi-output boost converter, which can share its total output between different series of output voltages for low and high power applications. In this scheme, over two switches for one output were required, and its control scheme was complicated. Besides, the corresponding output power cannot supply for individual loads independently. Chen *et al.*[3] investigated a multiple-output dc–dc converter with shared zero-current switching (ZCS) lagging leg. Although this converter with the soft-switching property can reduce the switching losses, this combination scheme with three full-bridge converters is more complicated, so that the achievement of high conversion efficiency is difficult and its cost is also increased.

A new generation of single input multiple output (SIMO) dc–dc converters has been developed based on boost and inverted topologies. However, in these configurations, loads are independently constructed except the negative output [4]. In the proposed SIMO converter, the techniques of soft switching and voltage clamping are adopted to reduce the switching and conduction losses via the utilization of a low voltage rated power switch with a small $R_{ds(on)}$. This project presents a newly designed SIMO dc–dc converter based on boost and inverted derived topologies with a coupled inductor. The

motivation of this project is to design a single input multiple output converter for increasing the conversion efficiency, voltage gain [5], reducing the complex control and saving the cost of manufacturing.

II. TOPOLOGY OVERVIEW AND ANALYSES

A. Block Diagram

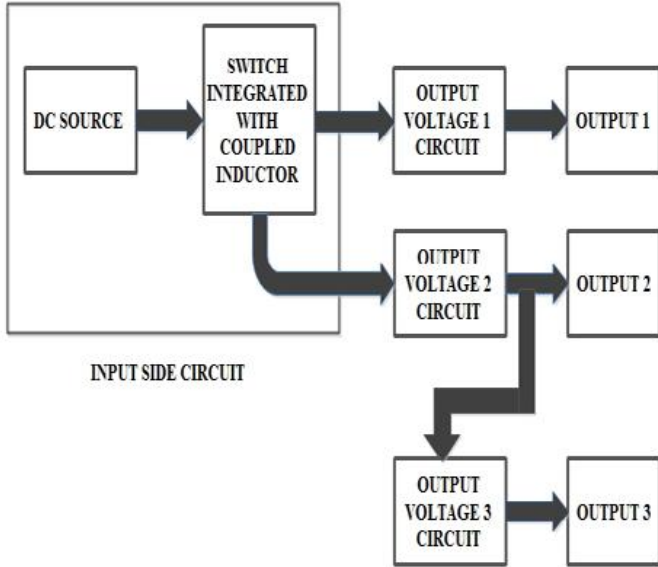


Fig.1 Proposed Single Input Multiple Output dc-dc converter Block Diagram

The Fig.1 shows the block diagram of Proposed Single Input Multiple Output dc-dc converter. The DC Source block consists of the dc input power source and a capacitor. The value of input is in the range of 12V. Switch Integrated with Coupled Inductor block consisting of a coupled inductor, a MOSFET switch and a diode. The coupled inductor primary has a series connected leakage inductor and a parallel connected magnetizing inductor. Output Voltage 1 Circuit consists of an auxiliary inductor, a diode and a filter capacitor. The value of output voltage 1 is 28V. Output Voltage 2 Circuit consists of a capacitor connected in series with the coupled inductor secondary and a diode connected in parallel with the above combination. In addition, the series connected diode and a filter capacitor is used. The value of output voltage 2 is 200V. Output Voltage 3 circuit consists of two MOSFET switches, two diodes and two capacitors.

B. Circuit Diagram & Description

The system configuration of the proposed SIMO converter topology to generate three different voltage levels from a single-input power source is depicted in Fig. 2. This SIMO converter contains six parts including an input side circuit (ISC), a clamped circuit, a coupled inductor secondary circuit, output voltage 1 circuit, output voltage 2 circuit and output voltage 3 circuit. The major symbol representations are

summarized as follows. V_{dc} (i_{dc}) and V_{o1} (i_{o1}) denote the voltages (currents) of the input power source and the output load at the input side voltage circuit and the output voltage 1 circuit, output voltage 2 circuit, a output voltage 3 circuit, respectively; C_1 , C_2 and C_3 are the clamped and coupled inductor secondary circuit capacitors in the clamped and coupled inductor secondary circuits respectively. L_p and L_s represent individual inductors in the primary and secondary sides of the coupled inductor respectively, where the primary side is connected to the input power source; L_{aux} is the auxiliary inductor. The main switch is expressed as S_1 in the ISC, S_2 and S_3 are the switches used in the output voltage circuit 3. The equivalent load in the output voltage circuit 1 is represented as R_{o1} , the output load is represented as R_{o2} in the output voltage circuit 2 and the output load is represented as R_{o3} in the output voltage circuit 3. The circuit diagram has the six diodes namely D_1 , D_2 , D_3 , D_4 , D_5 and D_6 respectively. The coupled inductor in Fig.2 can be modeled as an ideal transformer including the magnetizing inductor L_{mp} and the leakage inductor L_{kp} .

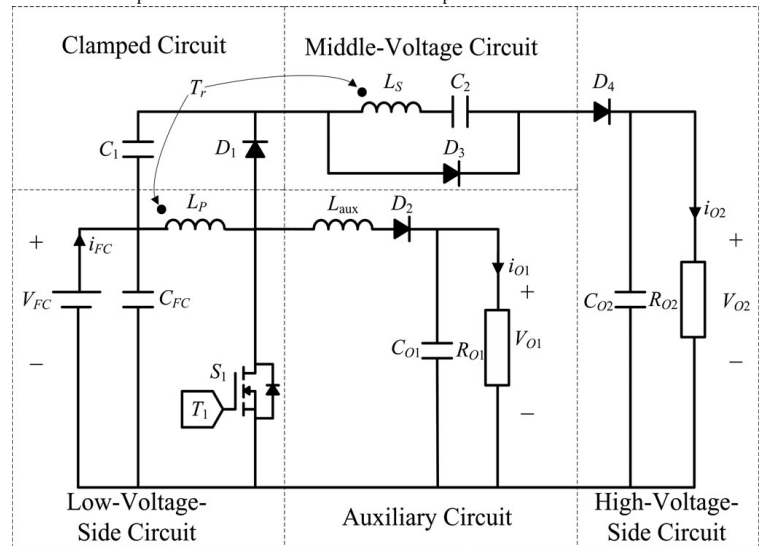


Fig.2 Proposed Single Input Multiple Output dc-dc converter Circuit Diagram

The turn's ratio N and coupling coefficient k of this ideal transformer are defined in equations 1 & 2 as,

$$N = N2/N1 \tag{1}$$

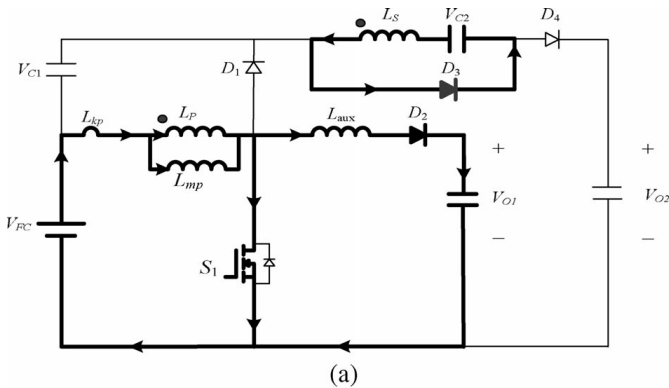
$$k = Lmp / (Lkp + Lmp) = Lmp/LP \tag{2}$$

where N_1 and N_2 are the winding turns in the primary and secondary sides of the coupled inductor. Because the voltage gain is less sensitive to the coupling coefficient and the clamped capacitor C_1 is appropriately selected to completely absorb the leakage inductor energy [6], the coupling coefficient could be simply set at unity to obtain $L_{mp} = L_p$.

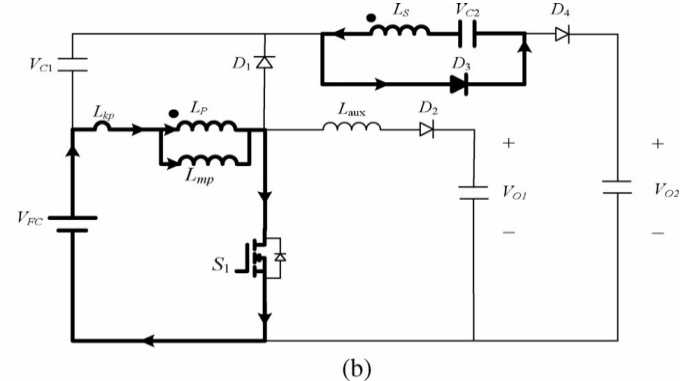
C. Modes of Operation

1) Mode 1 ($t_0 - t_1$)

In this mode, the main switch S_1 was turned ON for a span, and the diode D_4 turned OFF. Because the polarity of the windings of the coupled inductor Tr is positive, the diode D_3 turns ON. The secondary current iLs reverses and charges to the middle voltage capacitor C_2 . When the auxiliary inductor L_{aux} releases its stored energy completely, and the diode D_2 turns OFF, this mode ends.



2) Mode 2 ($t_1 - t_2$)

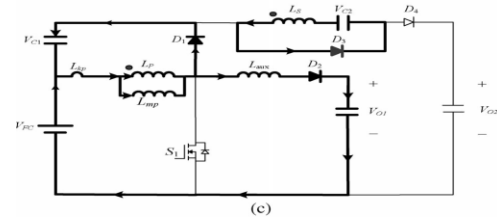


At time $t = t_1$, the main switch S_1 is persistently turned ON. Because the primary inductor L_p is charged by the input power source, the magnetizing current $iLmp$ increases gradually in an approximately linear way. At the same time, the secondary voltage vLs charges the middle-voltage capacitor C_2 through the diode D_3 . Although the voltage $vLmp$ is equal to the input voltage V_{FC} both at modes 1 and 2, the ascendant slope of the leakage current of the coupled inductor ($diLkp/dt$) at modes 1 and 2 is different due to the path of the auxiliary circuit. Because the auxiliary inductor

L_{aux} releases its stored energy completely, and the diode D_2 turns OFF at the end of mode 1, it results in the reduction of $diLkp/dt$ at mode 2.

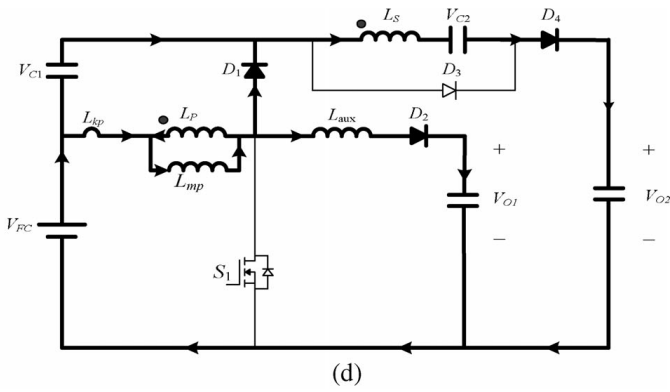
3) Mode 3 ($t_2 - t_3$)

The main switch S_1 is turned OFF. When the leakage energy still released from the secondary side of the coupled inductor, the diode D_3 conducts and releases the leakage energy to the capacitor C_2 . When the voltage across the main switch is higher than the clamped capacitor, the diode D_1 conducts to transmit the energy into the clamped capacitor C_1 . Thus, the current passes through the diode D_2 to supply the power for the output load in the output voltage 1 circuit. When the secondary side of the coupled inductor releases its leakage energy completely and the diode D_3 turns OFF. The closed loop of S_2 , C_3 and D_6 has been continued until the C_{02} completely discharged, this mode ends. The Fig.3(c) shows the operation of mode 3.



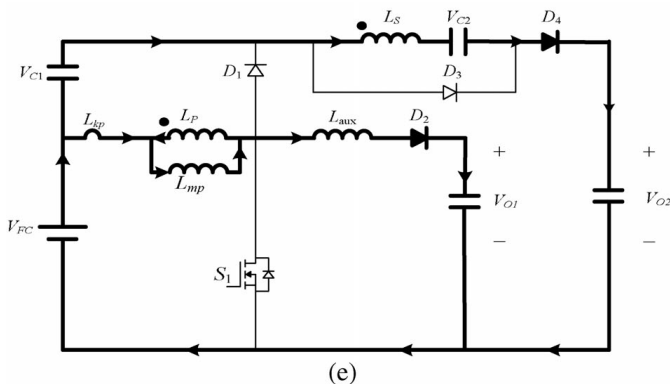
4) Mode 4 ($t_3 - t_4$)

As shown in Fig. (d), here the main switch S_1 is turned OFF. When the leakage energy has released from the primary side of the coupled inductor, the secondary current is induced in reverse from the energy of the magnetizing inductor L_{mp} through the ideal transformer and flows through the diode D_4 to the output voltage 2 circuit. At the same time, partial energy of the primary side leakage inductor L_{kp} is still persistently transmitted to the auxiliary inductor L_{aux} and the diode D_2 keeps conducting. Moreover, the current $I_{L_{aux}}$ passes through the diode D_2 to supply the power for the output load in the output voltage 1 circuit. Here S_1 is turned OFF and S_3 is turned ON, D_5 is forward biased and D_6 is reverse biased. C_3 is connected in series with S_3 , D_5 and C_{03} to form a closed loop and delivers the total voltage to C_{03} , so the output voltage across C_{03} is inverting voltage.



5) Mode 5 (t4-t5)

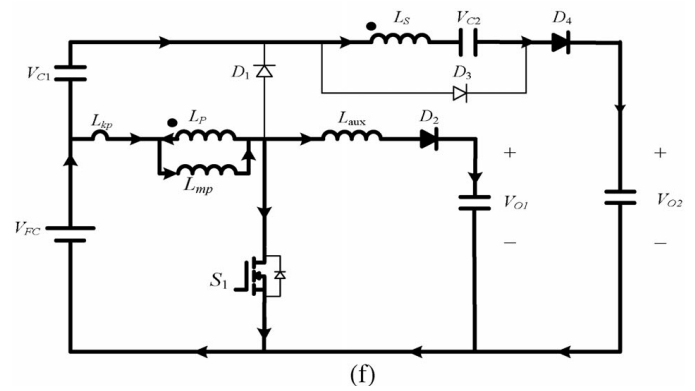
As depicted in Fig. (e), the main switch S_1 is turned OFF and the clamped diode D_1 turns OFF because the primary leakage current equals to the auxiliary inductor current. In this mode, the input power source, the primary winding of the coupled inductor and the auxiliary inductor L_{aux} connect in series to supply the power for the output load in the auxiliary circuit through the diode D_2 . At the same time, the input power source, the secondary winding of the couple inductor, the clamped capacitor C_1 and the capacitor C_2 connect in series to release the energy into the output voltage 2 circuit through the diode D_4 . Here S_3 is turned ON and S_1 is turned OFF, D_5 is forward biased and D_6 is reverse biased. C_3 is connected in series with S_3 , D_5 and C_{03} to form a closed loop and delivers the total voltage to C_{03} , so the output voltage across C_{03} is inverting voltage.



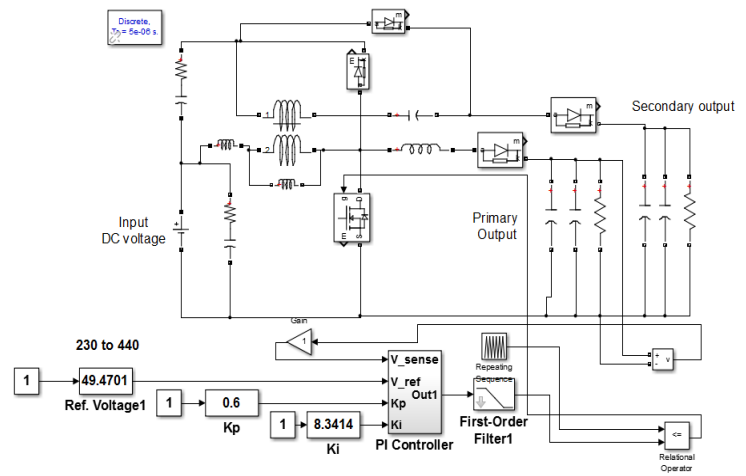
6) Mode 6 (t5-t6)

The operation of mode 6 is represented in Fig. (f). This mode begins when the main switch S_1 is triggered. The auxiliary inductor current needs time to decay to zero, the diode D_2 conducts. The input power source, the clamped capacitor C_1 , the secondary winding of the coupled inductor and the capacitor C_2 still connect loop and delivers the total voltage to C_{03} , so the output voltage across C_{03} is inverting voltage.

When the secondary current of the coupled inductor decays to zero, this mode ends.



III. SIMULINK MODEL AND RESULTS



The design of single input multiple output DC-DC converter is modeled using MATLAB/Simulink and the simulation model is shown in above Fig for 2 outputs.

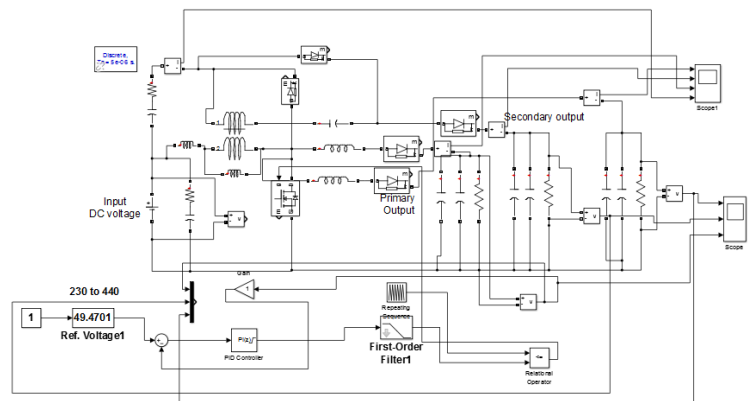


Fig. Simulink/MATLAB Model of SIMO DC-DC Converter for 3 outputs

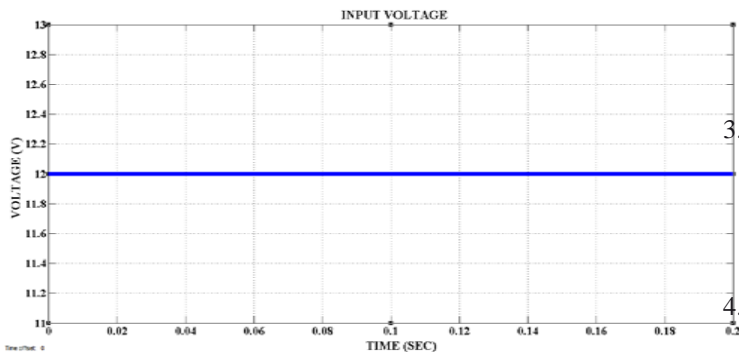


Fig. Input Voltage waveform of SIMO DC-DC Converter

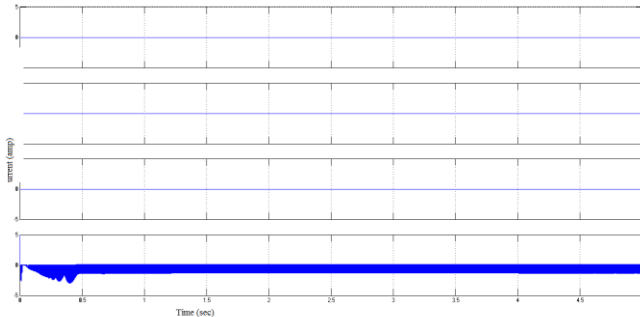


Fig. Input Current waveform of SIMO DC-DC Converter

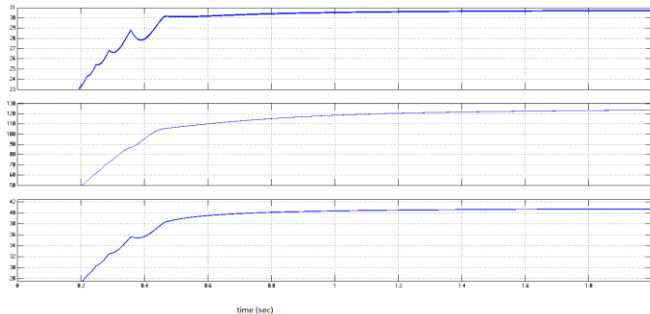


Fig. Output voltage waveform DC-DC Converter

IV. CONCLUSION

As per theory this study has successfully developed a high-efficiency SIMO dc-dc converter, and this coupled-inductor-based converter was applied well to a single-input power source plus two output terminals composed of an auxiliary battery module and a high-voltage dc bus. But from the result of simulation model it is quit not match with the third output of proposed theory circuitry and increased up to 130 volt with close loop control. It is due to fact that trial and error of choosing the value of coupled inductors

REFERENCES

1. Kirubakaran, S. Jain, and R. K. Nema, "DSP-controlled power electronic interface for fuel-cell-based distributed generation," *IEEE Trans. PowerElectron.*, vol. 26, no. 12, pp. 3853-3864, Dec. 2011.
2. B. Liu, S. Duan, and T. Cai, "Photovoltaic dc-building-

module-based BIPV system-concept and design considerations," *IEEE Trans. Power Electron.*, vol. 26, no. 5, pp. 1418-1429, May 2011.

3. M. Singh and A. Chandra, "Application of adaptive network-based fuzzy interference system for sensorless control of PMSG-based wind turbine with nonlinear-load-compensation capabilities," *IEEE Trans. Power Electron.*, vol. 26, no. 1, pp. 165-175, Jan. 2011.
4. C. T. Pan, M. C. Cheng, and C. M. Lai, "A novel integrated dc/ac converter with high voltage gain capability for distributed energy resource systems," *IEEE Trans. Power Electron.*, vol. 27, no. 5, pp. 2385-2395, May 2012.
5. S. D. Gamini Jayasinghe, D. Mahinda Vilathgamuwa, and U. K. Madawala, "Diode-clamped three-level inverter-based battery/supercapacitor direct integration scheme for renewable energy systems," *IEEE Trans. PowerElectron.*, vol. 26, no. 6, pp. 3720-3729, Dec. 2011.
6. H. Wu, R. Chen, J. Zhang, Y. Xing, H. Hu, and H. Ge, "A family of three- port half-bridge converters for a stand-alone renewable power system," *IEEE Trans. Power Electron.*, vol. 26, no. 9, pp. 2697-2706, Sep. 2012.
7. M. W. Ellis, M. R. Von Spakovsky, and D.J. Nelson, "Fuel cell systems: Efficient, flexible energy conversion for the 21 st century," *Proc. IEEE*, vol. 89, no. 12, pp. 1808-1818, Dec. 2001.
8. T. Kim, O. Vodyakho, and J. Yang, "Fuel cell hybrid electronic scooter," *IEEE Ind. Appl. Mag.*, vol. 17, no. 2, pp. 25-31, Mar./Apr. 2011.
9. F. Gao, B. Blunier, M. G. Simoes, and A. Miraoui, "PEM fuel cell stack modeling for real-time emulation in hardware-in-the-loop application," *IEEE Trans. Energy Convers*, vol. 26, no. 1, pp. 184-194, Mar. 2011.
10. P. Patra, A. Patra, and N. Misra, "A single-inductor multiple-output switcher with simultaneous buck, boost and inverted outputs," *IEEE Trans. Power Electron.*, vol. 27, no. 4, pp. 1936-1951, Apr. 2012.
11. A. Nami, F. Zare, A. Ghosh, and F. Blaabjerg, "Multiple-output DC-DC converters based on diode-clamped converters configuration: Topology and control strategy," *IET Power Electron.*, vol. 3, no. 2, pp. 197-208, 2010.
12. Y. Chen, Y. Kang, S. Nie, and X. Pei, "The multiple-output DC-DC converter with shared ZCS lagging leg," *IEEE Trans. Power Electron.*, vol. 26, no. 8, pp. 2278-2294, Aug. 2011.
13. R. J. Wai and R. Y. Duan, "High step-up converter with coupled inductor," *IEEE Trans. Power Electron.*, vol. 20, no. 5, pp. 1025-1035, Sep. 2005.

14. N. Mohan, T. M. Undeland, and W. P. Robbins, *Power Electronics: Converters, Applications, and Design*. New York: Wiley, 1995.
15. L. Schuch, C. Rech, H. L. Hey, H. A. Gründling, H. Pinheiro, and J. R. Pinheiro, "Analysis and design of a new high-efficiency bidirectional integrated ZVT PWM converter for DC-bus and battery-bank interface," *IEEE Trans. Ind. Appl.*, vol. 42, no. 5, pp. 1321-1332, Sep./Oct. 2006.
16. Y. Chen and Y. Kang, "A full regulated dual-output dc-dc converter with special-connected two transformers (SCTTs) cell and complementary pulsewidth modulation-PFM(CPWM-PFM)," *IEEE Trans. Power Electron.*, vol. 25, no. 5, pp. 1296-1309, May 2010.
17. J. K. Kim, S. W. Choi, and G. W. Moon, "Zero-voltage switching postregulation scheme for multioutput forward converter with synchronous switches," *IEEE Trans. Ind. Electron.*, vol. 58, no. 6, pp. 2378-2386, Jun. 2011.
18. L. Hang, S. Wang, Y. Gu, W. Yao, and Z. Lu, "High cross-regulation multioutput LLC series resonant converter with Magamp postregulator," *IEEE Trans. Ind. Electron.*, vol. 58, no. 9, pp. 3905-3913, Sep. 2011.
19. S. H. Cho, C. S. Kim, and S. K. Han, "High-efficiency and low-cost tightly regulated dual-output LLC resonant converter," *IEEE Trans. Ind. Electron.*, vol. 59, no. 7, pp. 2982-2991, Jul. 2012.
20. S. Karthik¹, C.Jegan², R.Ilango³ 'PG Student[PED], Department of EEE, M.A.M. School of Engineering, Siruganur, **Design of Single Input Multiple Output DC-DC Converter. Volume-4, Issue-2, April-2014, ISSN No.: 2250-0758 International Journal of Engineering and Management Research.**
21. **S. Anantha kumar¹** Second year PG scholar, Bannari Amman Institute of Technology, Sathyamangalam, India¹ **Modified Single Input Multiple Output DC-DC Converter. International Journal of Innovative Research in Science, An ISO 3297: 2007 Certified Organization, Volume 3, Special Issue 1, February 2014.**